

A high-performance wide-range beamline for elliptically polarized undulator source

S.-C. Chung,* Y.-F. Song, P.-C. Tseng, C.-C. Chen, C. T. Chen and K.-L. Tsang

Synchrotron Radiation Research Center, Hsinchu 300, Taiwan. E-mail: sc@alpha1.srrc.gov.tw

(Received 26 August 1997; accepted 29 October 1997)

A high-performance wide-range beamline has been designed for monochromatizing circularly polarized photons with energies from 10 to 1400 eV. A grazing SGM-based beamline with two entrance slits has been employed to optimize the performance. The degree of the circular polarization affected by the beamline optics has been analysed. The horizontal and vertical refocusing mirrors have been specially arranged to improve greatly the polarization degree in the low-energy region. By connecting this beamline to a high-efficiency elliptically polarized undulator, this beamline should be able to provide, in the entire energy range, intensive and high-resolution photons of a high degree of circular polarization.

Keywords: beamline; circular polarization.

1. Introduction

Circularly polarized synchrotron radiation in the VUV and soft X-ray range has attracted much demand lately because of its applications in circular intensity differential spectroscopy, magnetic circular dichroism (MCD), and spin-polarized photo-emission experiments (Maestre *et al.*, 1991; van der Lann & Thole, 1993; Chen, Sette, Ma & Modesti, 1990; Chen *et al.*, 1995; Heinzmann, 1987). Circularly polarized synchrotron radiation can be obtained from either the synchrotron radiation emitted above and below the electron orbit plane of a bending magnet, a linear undulator source with a quadruple reflector polarizer (Hochst *et al.*, 1995), or an elliptically polarized undulator (EPU) source. The degree of the circular polarization from the bending magnet can be as high as 90%; however, the flux of the circularly polarized beam is rather low because the photons from the bending magnet are mainly linearly polarized. In order to obtain a high degree of polarization, a beamline with grazing-incidence optics, such as the double-headed Dragon beamline (Chen, Sette & Smith, 1990), or with near-normal incidence optics, like the beamline BL28 at the Photon Factory (Kagoshima *et al.*, 1992), is used. The grazing angle ($<3^\circ$) design is good for photon throughput and the preservation of the polarization degree. However, the grazing angle has to be increased to optimize the energy resolution in the low-energy region. As the grazing-incidence angle is increased, the degree of circular polarization will be reduced. The normal incidence design and the quadruple reflection polarizer are inadequate for photon energies greater 100 eV, because the normal incidence in the former and the many optical reflections in the latter will severely degrade the overall photon flux.

A 3.9 m long Sasaki-type EPU with a magnet period of 5.6 cm is under construction at the SRRC (Wang *et al.*, 1996). This EPU undulator should be able to generate perfect circularly polarized photons with a flux similar to that of a conventional undulator. Therefore, all we need is to build a high-performance beamline for monochromatizing the circularly polarized photons. In the following, we report the analysis of the polarization change caused by the optical elements, and the design of a high-performance wide-range SGM beamline for the EPU source.

2. The photon polarization affected by the optics

The reflectance for each photon polarization component depends on the dielectric constant, ε , of the reflecting material and the incident angle of the photon beam. The reflectivity of the parallel polarized component, r_s , the reflectivity of perpendicularly polarized component, r_p , and the phase difference, Δ , between these two components can be calculated using the following Fresnel equations (Johnson & Smith, 1983):

$$r_p \exp(i\delta_p) = \frac{\varepsilon \cos \theta_i - (\varepsilon - \sin^2 \theta_i)^{1/2}}{\varepsilon \cos \theta_i + (\varepsilon - \sin^2 \theta_i)^{1/2}} \quad (1)$$

$$r_s \exp(i\delta_s) = \frac{\cos \theta_i - (\varepsilon - \sin^2 \theta_i)^{1/2}}{\cos \theta_i + (\varepsilon - \sin^2 \theta_i)^{1/2}} \quad (2)$$

$$\Delta = \delta_p - \delta_s. \quad (3)$$

The polarization degree can be significantly modified by each reflection, if the reflectance for each component is different. According to the Stokes parameter notation (Koide *et al.*, 1991), the initial Stokes parameters of the polarized light are written as $\mathbf{S}^{(x,y)}$. Then the final Stokes parameters after the polarized light reflected by an optical surface are given by the equation

$$\mathbf{S}^{(x,y)} = (1/2)(r_s^2 + r_p^2)R^{-1}(\alpha)M(\psi, \Delta)R(\alpha)\mathbf{S}^{(x,y)}, \quad (4)$$

where $R(\alpha)$ is the rotation matrix with a rotation angle of α and M is the Mueller matrix. These two matrices are given by

$$R(\alpha) = \begin{pmatrix} 1 & 0 & 0 & 0 \\ 0 & \cos 2\alpha & \sin 2\alpha & 0 \\ 0 & -\sin 2\alpha & \cos 2\alpha & 0 \\ 0 & 0 & 0 & 1 \end{pmatrix}$$

$$M(\psi, \Delta) = \begin{pmatrix} 1 & \cos 2\psi & 0 & 0 \\ \cos 2\psi & 1 & 0 & 0 \\ 0 & 0 & \sin 2\psi \cos \Delta & -\sin 2\psi \sin \Delta \\ 0 & 0 & \sin 2\psi \sin \Delta & \sin 2\psi \cos \Delta \end{pmatrix},$$

where $\psi = \arctan(r_p/r_s)$. The above equations will be used in this paper to calculate the reflectivity and the polarization degree.

3. Beamline optical design

There are three major goals for the EPU beamline design, namely high throughput, high energy resolution, and high circular polarization for the entire energy range from 10 to 1400 eV. To achieve these goals, we have adopted the wide-range SGM design proposed earlier for a bending-magnet source (Tseng *et al.*, 1998). The only modification is the arrangement of the pre-focusing and the re-focusing mirror systems.

The optical layout of the EPU beamline is shown in Fig. 1. Similar to a Dragon beamline design, the SGM is located between pre-focusing mirrors and the re-focusing mirrors. Grazing-incident angles are used to maximize the total photon throughput. Two entrance slits are used to achieve two different grating included angles, *i.e.* 160° for the low-energy branch (10–150 eV) and 174° for the high-energy branch (100–1400 eV). The first optical element, located at 15 m from the undulator source, will be one of the two vertical focusing mirrors, *i.e.* VFMH and VFML, depending on the energy branch to be used. These two mirrors have a spherical figure and a demagnification factor of ~ 5 . The VFMH (VFML) will deflect and focus the beam onto slit S_{1H} (S_{1L}). For VFML, an additional plane mirror is needed to form the 160° included angle. Six gratings are employed to cover the entire energy range. Gratings with ruling densities of 350, 800 and 1600 lines mm^{-1} are chosen for the low-energy branch, while gratings with ruling densities of 400, 800 and 1600 lines mm^{-1} are chosen for the high-energy branch.

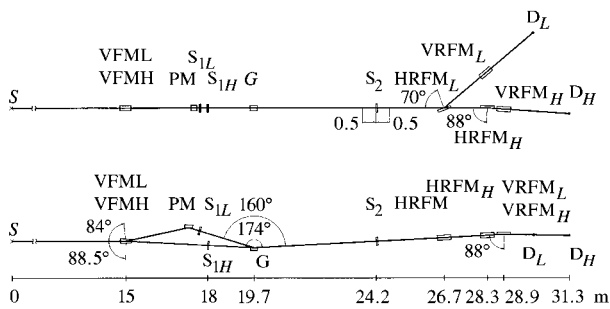


Figure 1
Optical layout of the wide-range EPU-SGM beamline.

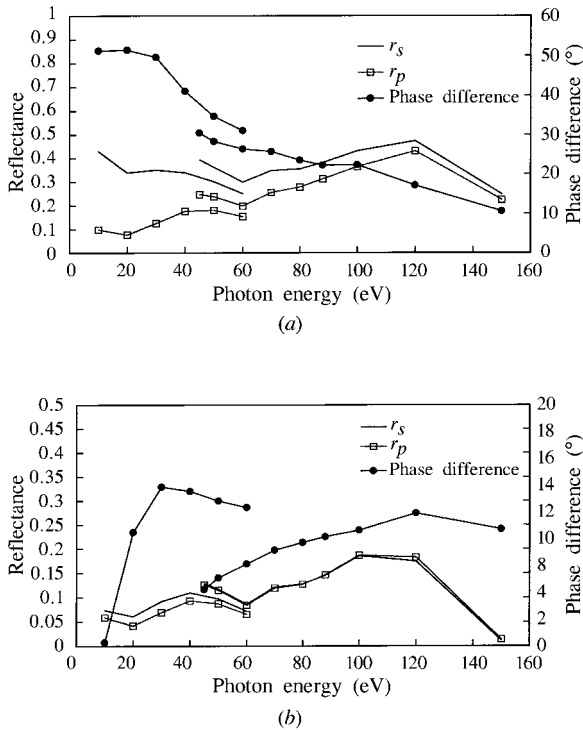


Figure 2
The final reflectance of the two different polarization components obtained in (a) the high-flux mode and in (b) the polarization-correcting mode.

In the normal operation, the horizontal and vertical refocusing mirrors, HRFM_H and VRFM_H , are used. The surface figure of both mirrors is cylindrical and the incident angle is 88° . The beam size at sample position, D_H , is less than $100 \times 100 \mu\text{m}$. In normal operation, a very high photon transmission can be obtained for the entire energy range and the circular polarization is completely preserved for the high-energy branch (100–1400 eV). To improve the circular polarization of the low-energy branch, two separate refocusing mirrors, HRFM_L and VRFM_L , have been employed. The incident angle of the HRFM_L is chosen to be 70° . This polarization correcting arrangement is only good for the low-energy branch. The total reflectance of the low-energy branch in the normal and the polarization correcting operations are shown in Figs. 2(a) and 2(b). The polarization degrees, calculated by (4), for the two operational modes in the entire energy range are shown in Figs. 3(a) and 3(b). The degree of circular polarization in the polarization correcting mode is better than 95%. At the polarization corrected mode, the photon flux will be reduced by a factor of two, but the polarization degree is substantially increased. The total photon transmission at the polarization correcting mode is about a few percent in the entire energy range (see Fig. 4). The energy resolving powers with both slits set at $10 \mu\text{m}$ are illustrated in Fig. 5. A resolving power of 20000 to 42000 can be reached for the low-energy branch, and of 7000 to 17000 for the high-energy branch.

4. Summary

A high-performance wide-range EPU-SGM beamline, covering photon energies from 10 to 1400 eV, has been designed. The grazing incidence is chosen to maximize the photon throughput and the circular polarization. Two entrance slits are employed to optimize the resolution. The polarization affected by the

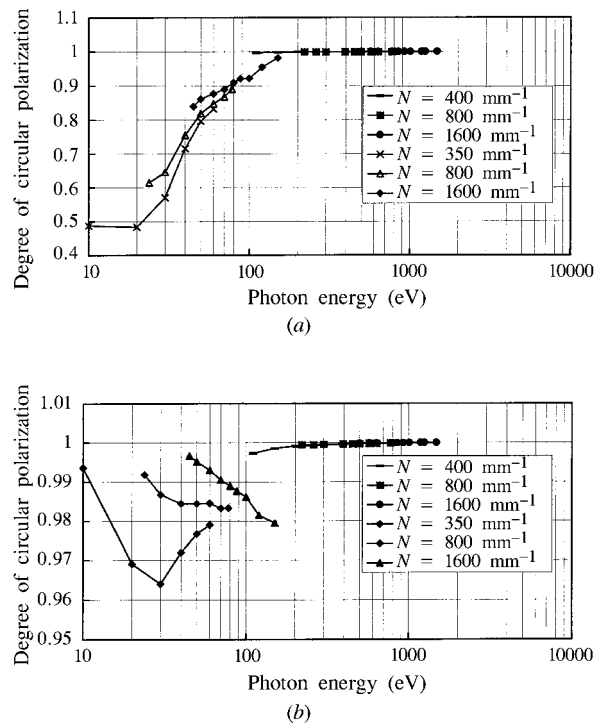


Figure 3
The circular polarization degree of photons obtained in (a) the high-flux mode and in (b) the polarization-correcting mode.

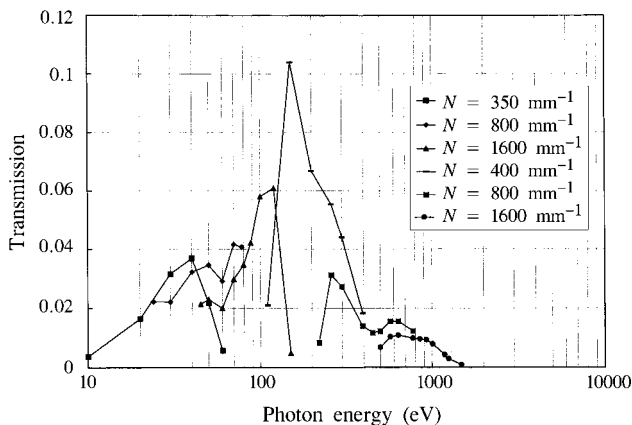


Figure 4
The transmission curves of the wide-range EPU-SGM beamline.

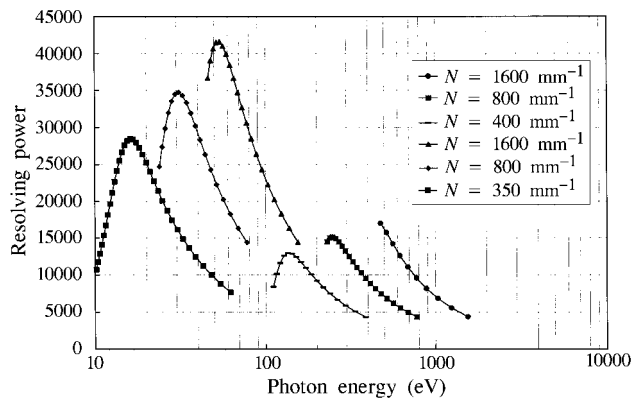


Figure 5
The resolving power of the wide-range EPU-SGM beamline.

reflecting surface has been analysed. Separate re-focusing mirror systems are devised to improve the polarization degree in the low-energy region. After the polarization correction, a circular polarization degree of over 95% is obtained for the entire energy range. A total throughput efficiency of a few percent with energy resolving powers between 10000 and 40000 is obtained. The beam size at the sample position is less than $100 \times 100 \mu\text{m}$.

We would like to thank Dr Ch. Wang for providing the information about the EPU source, and Dr M. Yuri for useful discussions on the polarization calculation.

References

Chen, C. T., Idzerda, Y. U., Kao, C.-C., Tjeng, L. H., Lin, H.-J. & Meigs, G. (1995). *Mater. Sci. Eng.* **B31**, 49–56.
 Chen, C. T., Sette, F., Ma, Y. & Modesti, S. (1990). *Phys. Rev. B*, **42**, 7262–7265.
 Chen, C. T., Sette, F. & Smith, N. V. (1990). *Appl. Opt.* **29**, 4535–4536.
 Heinzmann, U. (1987). *Phys. Scr.* **T17**, 77–88.
 Hochst, H., Bulicke, P., Nelson, T. & Middleton, F. (1995). *Nucl. Instrum. Methods*, **A347**, 107–114.
 Johnson, P. D. & Smith, N. V. (1983). *Nucl. Instrum. Methods*, **214**, 505–508.
 Kagoshima, Y., Muto, S., Miyahara, T., Koide, T., Yamamoto, S. & Kitamura, H. (1992). *Rev. Sci. Instrum.* **63**(1), 1289–1292.
 Koide, T., Shidara, T., Yuri, M., Kandara, N., Yamaguchi, K. & Fukutani, H. (1991). *Nucl. Instrum. Methods*, **A308**, 635–644.
 Lann, G. van der & Thole, B. T. (1993). *Phys. Rev. B*, **48**, 210–223.
 Maestre, M. F., Bustamante, C., Snyder, P., Rowe, E. & Hansen, R. (1991). *Proc. SPIE*, **1548**, 179–187.
 Tseng, P.-C., Chen, C.-C., Dann, T.-E., Chung, S.-C., Chen, C. T. & Tsang, K.-L. (1998). *J. Synchrotron Rad.*, **5**, 723–725.
 Wang, Ch., Chang, L. H., Chang, C. H., Chen, H. H., Fan, T. C., Hsu, K. T., Hsu, J. Y., Hwang, C. S., Lin, M. C. & Pan, K. T. (1996). *Proc. 5th EPAC*, pp. 2567–2569.